$$k_{ET} = \frac{2\pi(H_{AB})^2}{\hbar(4\pi\lambda kT)^{1/2}} \exp\left[\frac{-(\Delta G^\circ + \lambda)^2}{4\lambda kT}\right] \quad (1)$$

eq 1 is the electronic coupling matrix element for the ET reaction, and λ is the nuclear reorganization parameter. Analyses of the Ru(His-33)-Zn-cyt *c* and Ru(His-39)-Zn-cyt *c* data are shown in Figure 1. Only an increase in H_{AB}, as opposed to small variations in λ or ΔG°, can account for the fact that the Ru(His-39)-Zn-cyt *c* ET rates are 3 times the Ru(His-33)-Zn-cyt *c* rates over the 0.66-1.05 eV driving-force range.[26] The invariance of λ found in the ET* and ET^b reactions of the two proteins is consistent with theoretical considerations.[25,27,28]

The H_{AB} values for Ru(His-39)-Zn-cyt *c* (ET*, 0.24 cm^{-1}; ET^b, 0.18 cm^{-1}) are almost twice as large as those for Ru(His-33)-Zn-cyt *c* (ET*, 0.13 cm^{-1}; ET^b, 0.10 cm^{-1}).[21] It is likely that the electronic couplings in both proteins involve a superexchange mechanism in which electronic states of the intervening medium mix with localized donor states to produce a nonzero H_{AB}.[16,29,30] Calculations indicate that there are two relatively good pathways for ET from His-33 to the metalloporphyrin:[31] a 16-bond route to the Zn atom through His-18 that includes a 1.85-Å H bond between the Pro-30 carboxyl oxygen and the proton on the His-18 nitrogen and a 13-bond route ending with a 3.6-Å through-space contact between the δ-carbon of Pro-30 and a pyrrole carbon of the porphyrin. The shortest pathway from His-39 is a 13-bond route that includes a 2.4-Å H bond between the α-amino hydrogen atom of Gly-41 and the carboxyl oxygen of a propionate side chain on the porphyrin (Figure 2). Because a hydrogen bond is predicted[16] to be a better shortcut than a through-space jump, the 13-bond route from His-39 to the porphyrin should lead to stronger electronic coupling than the 13-bond pathway from His-33. The 16-bond bridge from His-33 to the Zn that includes an H bond may also provide better coupling than the 13-bond (Pro-30 through space to porphyrin) pathway. It should be only slightly less effective in coupling the ruthenium and porphyrin centers than the 13-bond pathway in Ru(His-39)-Zn-cyt *c*.[32]

Our work highlights the need for in-depth theoretical and experimental investigations of the possible role of hydrogen bonds in the pathways for long-range electron transfer through proteins. Systematic studies of electronic couplings in donor-(spacer)-acceptor molecules with variable H-bond connectors could be particularly valuable.

Acknowledgment. We thank David Beratan and Bruce Bowler for helpful discussions. M.J.T. acknowledges a postdoctoral fellowship from the National Institutes of Health. Research at the California Institute of Technology was supported by National Science Foundation Grant CHE88-22988. Research performed at Brookhaven National Laboratory was carried out under Contract DE-AC02-76CH00016 with the U.S. Department of Energy and supported by its Division of Chemical Sciences, Office of Basic Energy Sciences.

(25) Marcus, R. A.; Sutin, N. *Biochim. Biophys. Acta* **1985**, *811*, 265-322.
(26) The $Ru^{2+} \rightarrow Fe^{3+}$ ET rate in Ru_5(His-39)-Fe-cyt *c* ($\sim$170 s^{-1}; $-\Delta G^\circ$ = 0.17 eV; 22 °C)[23] also is substantially higher than that ($\sim$30 s^{-1}; $-\Delta G^\circ$ = 0.18 eV; 22 °C)[21] in Ru_5(His-33)-Fe-cyt *c*.
(27) (a) Brunschwig, B. S.; Ehrenson, S.; Sutin, N. *J. Am. Chem. Soc.* **1984**, *106*, 6858-6859. (b) Brunschwig, B. S.; Ehrenson, S.; Sutin, N. *J. Phys. Chem.* **1986**, *90*, 3657-3668.
(28) Dielectric continuum models of solvent reorganization predict that the outer-sphere contribution to λ (λ_o) will increase with donor-acceptor separation.[25,27] Modeling the Ru-Zn-cyt *c* systems as single spheres suggests that λ_o for the Ru(His-33)-Zn-cyt *c* reactions should be nearly the same as that for the Ru(His-39)-Zn-cyt *c* reactions (0.58 and 0.59 eV, respectively). The cyt *c* molecule was taken as a 17-Å sphere and the Ru-ammine group as a 6-Å sphere. These two interpenetrating spheres were enclosed by a third sphere of radius 17.6 Å for Ru(His-33)-Zn-cyt *c* and 18.2 Å for Ru(His-39)-Zn-cyt *c*. The Zn and Ru redox centers were taken as 6.0 and 14.6 Å from the center of the sphere, respectively, and separated from one another by 18.6 Å in Ru(His-33)-Zn-cyt *c*. The corresponding distances for the Ru(His-39)-Zn-cyt *c* model were 6.3, 15.2, and 19.3 Å. The dielectric constant of the sphere was taken as 1.8; the solvent was assigned a static dielectric constant of 78.54 and an optical dielectric constant of 1.78.
(29) The shortest direct distances between porphyrin carbon atoms and imidazole carbon atoms of His-33 (13.2 Å) and His-39 (13.0 Å) are much too long for any direct donor-acceptor interaction.[16] Calculations were made using BIOGRAF/111 version 1.34 (BIOGRAF was designed and written by S. L. Mayo, B. D. Olafson, and W. A. Goddard III). The structures of horse heart cytochrome *c* and its Ru(His-33) derivatives were built from the structure of the tuna protein by side-chain substitution and molecular mechanics energy minimization.[7a,7c,21] The structure of *C.k.* cytochrome *c* was generated from the structure of the tuna protein by side-chain substitution.[23] In both *C.k.* and horse heart proteins, an imidazole carbon on His-33 is 11.7 Å from an imidazole carbon of His-18, an axial ligand of the metalloporphyrin. This value has been used as the edge-to-edge distance in previous studies.[9,21] His-18 is not likely to be as strongly coupled to the porphyrin-localized donor and acceptor states as are carbon atoms of the porphyrin ring.[30] Hence, in comparing donor-acceptor coupling in Ru(His-33)-Zn-cyt *c* and Ru(His-39)-Zn-cyt *c*, distances to porphyrin carbon atoms have been used.
(30) (a) Gouterman, M. In *The Porphyrins*; Dolphin, D., Ed.; Academic Press: New York, 1978; Vol. III, pp 1-105. (b) Hanson, L. K. *Photochem. Photobiol.* **1988**, *47*, 903-921.
(31) Beratan, D. N.; Onuchic, J. N.; Betts, J. N.; Bowler, B. E.; Gray, H. B. *J. Am. Chem. Soc.*, submitted for publication.
(32) The H bonds in the His-33 (horse) and His-39 (*C.k.*) pathways are assumed to be the same as in the tuna protein. This assumption is reasonable, because the amino acids involved in these interactions (His-18, Pro-30, Gly-41) are conserved in the three proteins.[23]

Novel Pentacoordinate Anionic Silicate, [*o*-$C_6H_4(SiPhF_2)_2F]^-$,K^+·18-Crown-6, Containing a Bent Fluoride Bridge between Two Silicon Atoms

Kohei Tamao,* Takashi Hayashi, and Yoshihiko Ito*

Department of Synthetic Chemistry
Faculty of Engineering, Kyoto University
Kyoto 606, Japan

Motoo Shiro

Shionogi Research Laboratories, Shionogi & Co., Ltd.
Sagisu, Fukushima-ku, Osaka 553, Japan

Received October 30, 1989

Pentacoordinate anionic silicates have recently received much attention from structural and mechanistic points of view,[1] including the nature of bonding,[2] intramolecular ligand exchange,[3] intermolecular ligand exchange with tetracoordinate silanes,[4] enhanced reactivity toward nucleophiles,[5] and activation of the silicon-carbon bonds.[6] New aspects should further be accumulated.

(1) Review: (a) Tandura, St. N.; Alekseev, N. V.; Voronkov, M. G. *Top. Curr. Chem.* **1986**, *131*, 99-189. (b) Corriu, R. J. P.; Young, J. C. In *The Chemistry of Organic Silicon Compounds*; Patai, S., Rappoport, Z., Ed.; John Wiley: Chichester, 1989; p 1241.
(2) For example: (a) Sini, G.; Hiberty, P. C.; Shaik, S. S. *J. Chem. Soc., Chem. Commun.* **1989**, 772. (b) Reed, A. E.; Schleyer, P. v. R. *Chem. Phys. Lett.* **1987**, *133*, 553. (c) Damrauer, R.; Burggraf, L. W.; Davis, L. P.; Gordon, M. S. *J. Am. Chem. Soc.* **1988**, *110*, 6601. (d) Harland, J. J.; Payne, J. S.; Day, R. O.; Holmes, R. R. *Inorg. Chem.* **1987**, *26*, 760. (e) Kira, M.; Sato, K.; Kabuto, C.; Sakurai, H. *J. Am. Chem. Soc.* **1989**, *111*, 3747.
(3) Recent papers: (a) Johnson, S. E.; Day, R. O.; Holmes, R. R. *Inorg. Chem.* **1989**, *28*, 3182. (b) Johnson, S. E.; Payne, J. S.; Day, R. O.; Holmes, J. M.; Holmes, R. R. *Inorg. Chem.* **1989**, *28*, 3190. (c) Johnson, S. E.; Deiters, J. A.; Day, R. O.; Holmes, R. R. *J. Am. Chem. Soc.* **1989**, *111*, 3250. (d) Damrauer, R.; O'Connell, D.; Danahey, S. E.; Simon, R. *Organometallics* **1989**, *8*, 1167. (e) Damrauer, R.; Danahey, S. E. *Organometallics* **1986**, *5*, 1490. (f) Stevenson, W. H., III; Wilson, S.; Martin, J. C.; Farnham, W. B. *J. Am. Chem. Soc.* **1985**, *107*, 6340.
(4) (a) Brownstein, S. *Can. J. Chem.* **1980**, *58*, 1407. (b) Marat, R. K.; Janzen, A. F. *Can. J. Chem.* **1977**, *55*, 1167, 3845. (c) Klanberg, F.; Muetterties, E. L. *Inorg. Chem.* **1968**, *7*, 155.
(5) (a) Carre, F.; Cerveau, G.; Chuit, C.; Corriu, R. J. P.; Reye, C. *Angew. Chem., Int. Ed. Engl.* **1989**, *28*, 489 and references cited therein. (b) Sato, K.; Kira, M.; Sakurai, H. *J. Am. Chem. Soc.* **1989**, *111*, 6429. (c) Hayashi, T.; Matsumoto, Y.; Kiyoi, T.; Ito, Y.; Kohra, S.; Tominaga, Y.; Hosomi, A. *Tetrahedron Lett.* **1988**, *29*, 5667. (d) Webster, O. W.; Hertler, W. R.; Sogah, D. Y.; Farnham, W. B.; RajanBabu, T. V. *J. Am. Chem. Soc.* **1983**, *105*, 5706. See also ref 3c.

0002-7863/90/1512-2422$02.50/0

Scheme I[a]

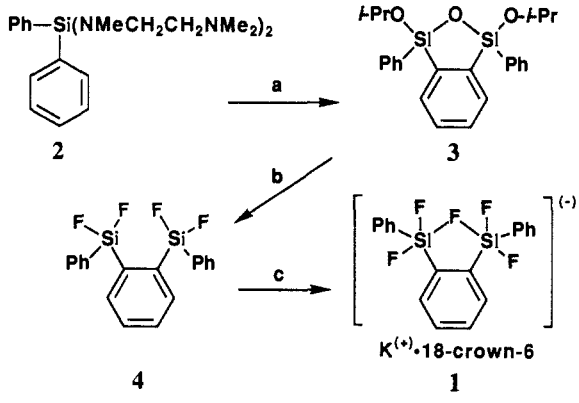

[a] (a) (1) *t*-BuLi, 0 °C to room temperature, 2 h. (2) $PhSiCl_3$, 50 °C, 3 h. (3) *i*-PrOH, room temperature, 12 h. (4) Et_3N, H_2O (1 equiv) (57% yield). (b) $HBF_4{\cdot}Et_2O$, CH_2Cl_2, 0 °C, 12 h (88% yield). (c) KF (1 equiv), 18-crown-6 (1 equiv), toluene, room temperature, 20 h (64% yield).

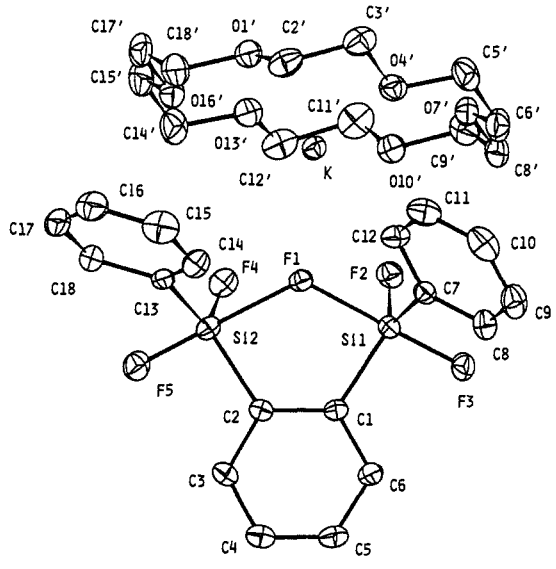

Figure 1. X-ray structure of **1**. Selected distances (angstroms) and angles (degrees): Si1–F1, 1.898 (4); Si1–F2, 1.616 (4); Si1–F3, 1.657 (4); Si1–C1, 1.877 (5); Si1–C7, 1.879 (5); Si2–F1, 2.065 (4); Si2–F4, 1.601 (4); Si2–F5, 1.638 (4); Si2–C2, 1.867 (5); Si2–C13, 1.871 (5); K–F1, 3.042 (3); K–F2, 2.780 (3); K–F4, 3.073 (3); Si1–F1–Si2, 119.7 (2); F1–Si1–F2, 82.3 (2); F1–Si1–C1, 85.0 (2); F1–Si1–C7, 90.4 (2); F3–Si1–F2, 91.4 (2); F3–Si1–C1, 95.3 (2); F3–Si1–C7, 96.1 (2); F1–Si1–F3, 172.6 (2); F2–Si1–C1, 124.0 (2); F2–Si1–C7, 117.7 (2); C1–Si1–C7, 116.7 (2); F1–Si2–F4, 80.9 (2); F1–Si2–C2, 81.7 (2); F1–Si2–C13, 87.4 (2); F5–Si2–F4, 94.6 (2); F5–Si2–C2, 97.7 (2); F5–Si2–C13, 97.4 (2); F1–Si2–F5, 174.5 (2); F4–Si2–C2, 119.1 (2); F4–Si2–C13, 115.6 (2); C2–Si2–C13, 121.3 (2).

We report herein the first synthesis, X-ray crystallography, and solution spectral behavior of a novel pentacoordinate anionic silicate, $[o\text{-}C_6H_4(SiPhF_2)_2F]^-,K^+{\cdot}$18-crown-6 (**1**), which contains a fluoride ion chelated by two silyl groups. The synthetic route is illustrated in Scheme I. Thus, an ortho-lithiated species[7] of a diaminodiphenylsilane **2** was quenched by $PhSiCl_3$, followed by alcoholysis with 2-propanol to give a cyclic *o*-disilylbenzene derivative **3**, which was then treated with fluoroboric acid to form the precursor, *o*-bis(difluorophenylsilyl)benzene (**4**). Treatment of **4** with spray-dried KF[8] and 18-crown-6 in toluene at room temperature for 20 h gave white crystalline solids, which were recrystallized from dry THF to give pure **1**; mp 149.5–150.5 °C dec. Anal. Calcd for $C_{30}H_{38}O_6F_5Si_2K$: C, 52.61; H, 5.59; F, 13.87. Found: C, 52.35; H, 5.55; F, 14.06,

Table I. ^{13}C, ^{19}F, and ^{29}Si Nuclear Magnetic Resonance Data for **1** at Room Temperature

	chemical shift: δ, ppm (multiplicity, coupling constant, assignments)
$^{13}C\{H\}$[a]	70.71 (singlet, 18-crown-6)
	127.29 (singlet, C9, C11, C15, C17)
	128.90 (singlet, C10, C16)
	129.62 (singlet, C4, C5)
	136.75 (sextet, $^3J_{CF}$ = 2.64 Hz, C8, C12, C14, C18)
	138.49 (sextet, $^3J_{CF}$ = 3.85 Hz, C3, C6)
	142.02 (sextet, $^2J_{CF}$ = 19.06 Hz, C1, C2)[b]
	149.03 (sextet, $^2J_{CF}$ = 16.86 Hz, C7, C13)[b]
^{19}F[c]	−117.3 (broad singlet)
^{29}Si[d]	−90.03 (sextet, J_{SiF} = 134.74 Hz, Si1, Si2)

[a] Measured at 100.59 MHz, in acetone-d_6; δ referenced to acetone-d_6 (δ 29.8 ppm). [b] Tentatively assigned on the basis of δ 148.40 ppm of ipso carbons in $[Ph_2SiF_3]^-$. [c] Measured at 188.15 MHz in acetone-d_6; standard, $CFCl_3$ (δ 0 ppm). [d] Measured at 39.73 MHz, in acetone-d_6; standard, TMS (δ 0 ppm).

The X-ray structure of **1** is shown in Figure 1,[9] which confirms the presence of a bridging fluoride ion between two silicon atoms. Significant structural features are as follows. (1) The geometry about the silicon atoms is nearly trigonal bipyramidal, with two fluorine atoms occupying the apical positions, but the molecular distortion modes differ from those of pentacoordinate silicates so far reported.[10] Thus, the Si1 and Si2 atoms are displaced 0.131 and 0.205 Å out of the F2–C1–C7 plane and the F4–C2–C13 plane to the direction of F3 and F5, respectively,[11] indicating residual tetrahedral character in the Si1–C1–C7–F2–F3 and Si2–C2–C13–F4–F5 moieties; the tetrahedral character is larger in the latter than in the former. (2) The fluoride bridge is unsymmetrical, with the bond lengths F1–Si1 = 1.898 (4) Å and F1–Si2 = 2.065 (4) Å, respectively. It should be noted that these apical Si–F bonds are the longest ever found in pentacoordinate silicates.[12] The shortest apical Si–F bonds, Si1–F3 = 1.657 (4) Å and Si2–F5 = 1.638 (4) Å,[12] and the shortest equatorial bond, Si2–F4 = 1.601 (4) Å, for the $[R_2SiF_3]^-$ series are also noted.[11] (3) The unsymmetrical fluoride F1 bridge is bent, with the angle Si1–F1–Si2 = 119.7 (2)°. The five-membered ring is puckered, and the angle between the Si1–C1–C2–Si2 plane and the Si1–F1–Si2 plane is 34,0°. (4) Of two possible stereoisomers, only the cis isomer has been found. The main reason may reside in the interaction between the countercation K^+ and *three* fluorine atoms, F1, F2, and F4. Significantly, the K^+ is in close proximity to one equatorial fluorine, F2, K–F2 = 2.780 (3) Å, rather than

(6) (a) Tamao, K. In *Organosilicon and Bioorganosilicon Chemistry*; Sakurai, H., Ed.; Ellis Horwood: Chichester, 1985; pp 231–242. (b) Tamao, K.; Akita, M.; Maeda, K.; Kumada, M. *J. Org. Chem.* **1987**, *52*, 1100. (c) Kuwajima, I.; Nakamura, E.; Hashimoto, K. *Tetrahedron* **1983**, *39*, 975. (d) Cerveau, G.; Chuit, C.; Corriu, R. J. P.; Reye, C. *J. Organomet. Chem.* **1987**, *328*, C17. (e) Sheldon, J. C.; Hayes, R. N.; Bowie, J. H.; DePuy, C. H. *J. Chem. Soc., Perkin Trans. 2* **1987**, 275. (f) Yamamoto, Y.; Takeda, Y.; Akiba, K. *Tetrahedron Lett.* **1989**, *30*, 725. (g) Hatanaka, Y.; Hiyama, T. *J. Org. Chem.* **1989**, *54*, 268.

(7) Selective ortho-metalation directed by amino groups on silicon in arylsilanes: Tamao, K.; Tsutsumi, Y.; Yao, H.; Abe, H.; Hayashi, T.; Ito, Y. *Tetrahedron Lett.* Submitted for publication.

(8) Commercially available from Wako Pure Chemical Ind., Ltd., Osaka, Japan, and Aldrich Chemical Co., Ltd.

(9) Crystal data: triclinic, space group *P*1, a = 10.072 (3) Å, b = 11.158 (4) Å, c = 8.500 (3) Å; α = 113.79 (3)°, β = 108.02 (2)°, γ = 64.89 (3)°; V = 829.2 (5) Å^3, Z = 1; d_{calcd} = 1.372 g cm^{-3}; μ = 26.7 cm^{-1}; Cu Kα radiation (λ = 1.541 78 Å). The structure was solved by direct methods and refined by block-diagonal least squares to R = 0.034 and R_w = 0.047 for 2462 observed reflections [$F_o > 3\sigma(F_o)$]. Further details are provided as supplementary material.

(10) The known pentacoordinate silicates generally deform from trigonal bipyramidal to tetragonal pyramidal on the Berry pseudorotation coordinate.[3]

(11) In most of the known pentacoordinate anionic silicates, the silicon atom is nearly in the equatorial plane; e.g., Si atoms in $[Ph(p\text{-}XC_6H_4)SiF_3]^-$ (X = CF_3, Me, OMe, NMe_2) are deviated only about 0.02–0.03 Å out of the equatorial plane: Tamao, K.; Hayashi, T.; Ito, Y.; Shiro, M. *Organometallics*, to be submitted.

(12) In a series of $[R_2SiF_3]^-$, the longest apical Si–F, 1.729 (6) Å, is found in $[Mes_2SiF_3]^-$,[3c] the shortest apical Si–F, 1.682 (4) Å, in $[t\text{-}BuPhSiF_3]^-$,[3b] and the shortest equatorial Si–F, 1.621 (4) Å, in $[MePhSiF_3]^-$.[2d] The longest among shorter K–F distances found in a series of $[R_2SiF_3]^-,K^+{\cdot}$18-crown-6 may be 2.703 (6) Å in $[Xyl_2SiF_3]^-$.[2b]

to the apical F1, K-F1 = 3.042 (3) Å (and to the other equatorial fluorine, F4, K-F4 = 3.073 (3) Å), in contrast to most of the known fluorosilicates, where the K^+ ion interacts with *two* fluorine atoms, having a shorter distance to the apical than to the equatorial fluorine. It should be further noted that the shortest K-F2 distance seems to be longest among the shortest ones ever found in fluorosilicates,[12] demonstrating looser K-F interaction in the present case.

^{13}C, ^{19}F, and ^{29}Si NMR studies have shown remarkable behavior of **1** in solution. The data recorded at room temperature are given in Table I. Significantly, while the ^{19}F NMR shows a broad *singlet*, the ^{29}Si spectrum exhibits a *sextet* for two silicon atoms, and the ^{13}C NMR spectrum shows two *sextets* due to two kinds of ipso carbons, C1 (=C2) and C7 (=C13), and two narrower *sextets* due to two kinds of ortho carbons, C3 (=C6) and C8 (=C12, C14, C18). These data clearly demonstrate that all the five fluorine atoms are equivalent on the NMR time scale owing to rapid intramolecular exchange processes. Fast fluoride transfer between tetracoordinate and pentacoordinate silicon atoms is supported by comparison of the chemical shift and coupling constant data of **1** with those of typical tetracoordinate silanes such as Ph_2SiF_2 and pentacoordinate silicates such as $[Ph_2SiF_3]^-$. Firstly, the Si chemical shift (δ -90.03 ppm) of **1** is intermediate between those of Ph_2SiF_2 (δ -29.00 ppm) and $[Ph_2SiF_3]^-$ (δ -109.55 ppm). Secondly, the Si-F coupling constant (J_{SiF} = 134.74 Hz) is smallest in comparison with those of Ph_2SiF_2 ($^1J_{SiF}$ = 291.2 Hz) and $[Ph_2SiF_3]^-$ ($^1J_{SiF}$ = 238.06 Hz) and is comparable with the calculated average value (143 Hz) on the assumption that $^1J_{SiF}$ = 238 Hz (×3F) and $^4J_{SiF}$ = 0 Hz (×2F).

Variable-temperature ^{19}F NMR studies have shown two consecutive processes for the fluorine exchange. At -80 °C, three signals are observed due to the bridging F1 (δ -70.11 ppm), apical F3 and F5 (δ -115.69 ppm), and equatorial F2 and F4 (δ -142.15 ppm).[13] The first two signals coalesce at -33 °C, the last remaining as a broad singlet, and coalescence of all signals is observed at -16 °C. The first process should be attributable to a rapid exchange of the bridging fluorine atom between two silicon atoms, and the second, slower process is the intramolecular ligand exchange by the Berry pseudorotation,[3] the energy barriers being estimated to be 9.2 and 10.2 kcal/mol, respectively. Since the latter value is in the range of energy barriers reported for monosilicates $[Ar_2SiF_3]^-$,[3] the pseudorotation process appears to be little influenced by the *o*-silyl group in the present case.

In summary, **1** represents a novel case where solution and solid-state structures are not the same and serves as a good model (1) for nucleophilic attack on a tetrahedral silane by a fluoride ion—geometries of both silicon atoms are in the middle of the reaction coordinate for the tetrahedral to trigonal-bipyramidal transformation—and (2) for *intermolecular* fluorine exchange processes between pentacoordinate fluorosilicate and tetracoordinate silane,[4] which have frequently been spectroscopically detected. Furthermore, the high stability of **1** suggests utilization of the precursor **4** as a new chelating trapping agent for anions such as H^-, RO^-, and Cl^- as well as F^-.[14] We are currently engaged in study along this line and the synthesis of unsymmetrical *o*-disilyl analogues of **1**.

Supplementary Material Available: Synthesis, physical constants, and spectral and analytical data on compounds **1**, **3**, and **4**, ^1H, ^{13}C, ^{19}F, and ^{29}Si NMR spectra at room temperature and temperature-dependent ^{19}F NMR spectra of **1**, and tables of crystallographic data, atomic coordinates, bond lengths and angles, and anisotropic thermal parameters for **1** (14 pages). Ordering information is given on any current masthead page.

(13) At -80 °C, three small signals appeared near the major signals, possibly due to the trans isomer.

(14) Selective anion complexation has recently been studied by employing Lewis acidic metal compounds. 1,8-Diborylnaphthalenes and 1-boryl-8-silylnaphthalenes: (a) Katz, H. E. *J. Org. Chem.* **1985**, *50*, 5027. (b) Katz, H. E. *J. Am. Chem. Soc.* **1986**, *108*, 7640. (c) Katz, H. E. *Organometallics* **1987**, *6*, 1134. Si macrocycles: (d) Jung, M. E.; Xia, H. *Tetrahedron Lett.* **1988**, *29*, 297. Sn macrocycles: (e) Newcomb, M.; Horner, J. H.; Blanda, M. T.; Squattrito, P. J. *J. Am. Chem. Soc.* **1989**, *111*, 6294. Hg macrocycles: (f) Wuest, J. D.; Zacharie, B. *J. Am. Chem. Soc.* **1987**, *109*, 4714. Lehn's anion cryptates: (g) Lehn, J.-M. *Angew. Chem., Int. Ed. Engl.* **1988**, *27*, 89. (h) Dietrich, B.; Lehn, J.-M.; Guilhem, J.; Pascard, C. *Tetrahedron Lett.* **1989**, *30*, 4125.

Does the Hydroxycarbonyl Anion Convert to the Formate Anion in the Gas Phase? A Potential Surface Map of the H^-/CO_2 System

John C. Sheldon* and John H. Bowie

Departments of Chemistry, The University of Adelaide Adelaide, South Australia 5001, Australia

Received October 30, 1989

Deprotonation of formic acid with HO^- in the gas phase yields mainly the formate ion (HCO_2^-) together with a lesser amount of the hydroxycarbonyl anion ($HOCO^-$).[1] Ab initio calculations suggest that HCO_2^- is the more stable of the two by some 160 kJ mol^{-1}.[2] It has been suggested[1] from a consideration of the charge reversal[3] spectra of these two ions[1,4] that slow interconversion of the two ions could occur on collisional activation.[5]

A potential energy surface map of the hydride ion–carbon dioxide system is shown in Figure 1; particular structures represented by the surface are shown in Scheme I. The map depicts the variation in energy as a function of two system coordinates, viz., (i) the distance of H^- from O_1 and (ii) the angle H^- makes to the O_1–C bonding direction. The coordinates are chosen to best represent the interconversion of the two adducts formed between H^- and carbon dioxide.[6,7] The map was constructed from 160 points. Each point was optimized at the RHF/6-31+G* level and energy refined by a single point calculation at RMP2-FC/6-311++G**//RHF/6-31+G* (GAUSSIAN 86).[8,9] Energies (with

(1) Burgers, P. C.; Holmes, J. L.; Szulejko, J. E. *Int. J. Mass Spectrom. Ion Processes* **1984**, *57*, 159.

(2) MP2/4-31+G//4-31+G calculations: Chandrasekhar, J.; Andrade, J. G.; Schleyer, P. v. R. *J. Am. Chem. Soc.* **1981**, *103*, 5612. For a recent calculation on HCO_2^- (MP2/6-31G*), see: Masamura, M. *Theor. Chim. Acta* **1989**, *75*, 433.

(3) Bowie, J. H.; Blumenthal, T. *J. Am. Chem. Soc.* **1975**, *97*, 2959. Szulejko, J. E.; Bowie, J. H.; Howie, I.; Beynon, J. H. *Int. J. Mass Spectrom. Ion Phys.* **1980**, *13*, 76.

(4) Bursey, M. M.; Harvan, D. J.; Parker, C. E.; Pedersen, L. G.; Hass, J. R. *J. Am. Chem. Soc.* **1979**, *101*, 5489.

(5) Such a possibility has been considered in cognate systems: e.g., (a) $MeCO^-$ does not convert (experimentally) to $(CH_2CHO)^-$ because of a more favorable channel of $MeCO^-$ to yield Me^- + CO (Downard, K. M.; Sheldon, J. C.; Bowie, J. H. *Int. J. Mass Spectrom. Ion Processes* **1988**, *86*, 217), and (b) in contrast, the ions $MeCO_2^-$ and $(CH_2CO_2H)^-$ are interconvertible under conditions of collisional activation (O'Hair, R. A. J.; Gronert, S.; DePuy, C. H.; Bowie, J. H. *J. Am. Chem. Soc.* **1989**, *111*, 3105).

(6) The two oxygen atoms are not equivalent, O_1 being of fixed origin and O_2 relaxing up and down about the O_1–C vector. Thus the map is not bilaterally symmetrical, although some parts are strictly stereochemically equivalent.

(7) The optimum geometry of H^-/CO_2 adducts are consistently coplanar at the RHF level. It is assumed that the system is coplanar throughout the variation of hydride coordinates. Of the remaining four molecular coordinates which the two-dimensional map cannot show, only three are significant, i.e., the O_1–C bonding distance, the C–O_2 distance, and the OCO angle.

(8) Frisch, M.; Binkley, J. S.; Schlegel, H. B.; Raghavachari, K.; Martin, R.; Stewart, J. J. P.; Bobrowicz, F.; DeFrees, D.; Seeger, R.; Whiteside, R.; Fox, D.; Fluder, E.; Pople, J. A. *GAUSSIAN 86, Release C*; Carnegie Mellon University: Pittsburg, PA.

(9) A number of other optimizations were carried out at the RHF/6-311++G** level: these geometries and their subsequent MP2 energies are little different from those derived from RHF/6-31+G* optimizations. Optimized geometries are thus insensitive to the presence of diffuse and polarization functions on the hydride ion. However, gridding the MP2 energies against hydride coordinates effectively gives an MP2/6-311++G** variational location of adducts and saddlepoints.

(10) Geometry (RHF/6-31+G*): C_s (singlet state); O_1C (1.4225 Å), CO_2 (1.2192 Å), O_1H (0.9579 Å), O_1CO_2 (111.2793°), CO_1H (105.6417°). Energy (RMP2-FC/6-311++G**//RHF/6-31+G*), -188.74241 au.

(11) (a) The anti conformer of **1**: C_s (singlet state); O_1C(1.4541 Å), CO_2 (1.2036 Å), O_1H (0.9452 Å), O_1CO_2 (111.0766°), CO_1H (104.2624°). Energy, -188.740 21 au. (b) The syn conformer is the more stable of the two by 5 kJ mol^{-1}; presumably this is due to the attraction of H and O_2.

(12) Saddlepoint A: O_1C (1.27 Å), CO_2 (1.21 Å), CH (1.20 Å), O_1H (1.20 Å), O_1CO_2 (130°).

0002-7863/90/1512-2424$02.50/0